Lattice QCD Study of Excited Hadron Resonances

Colin Morningstar
Carnegie Mellon University

Effective Field Theories and Lattice Gauge Theory
TUM Insitute for Advanced Study, Garching, Germany

May 21, 2016

- spectroscopy resurgence due to discovery of unexpected charmonium *XYZ* states
- GlueX and JLab Hall D search for hybrids, other exotics

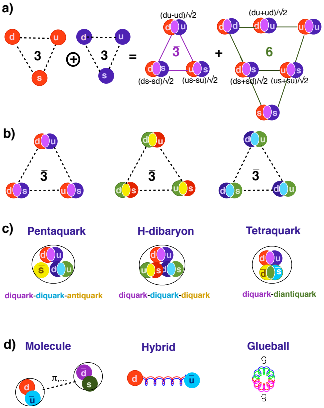

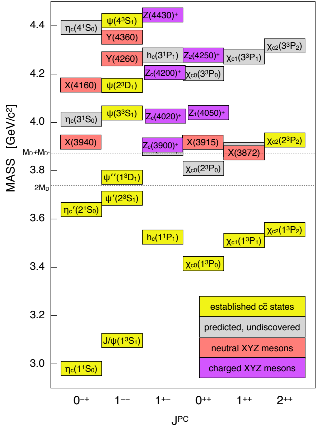

Key Points

- crucial role of interpolating operators for excited-state studies in lattice QCD
- lower-lying multi-hadron levels must be dealt with
- need to handle many quark lines: stochastic LapH method

- level identification using interpolating operators
- finite-volume energies $\Rightarrow$ hadron resonance properties: masses, decay widths

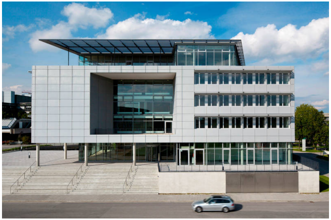

- focus: large 32^3 anisotropic lattices, $m_\pi \sim 240$ MeV
- scattering phase shifts from finite-volume energies
- need for effective Hamiltonian approach
- tetraquark operators

Excited states from correlation matrices

- in finite volume, energies are discrete (neglect wrap-around)

$$C_{ij}(t) = \sum_n Z_i^{(n)} Z_j^{(n)*} \; e^{-E_n t}, \qquad Z_j^{(n)} = \langle 0|\; O_j \;|n\rangle$$

- not practical to do fits using above form
- define new correlation matrix $\widetilde{C}(t)$ using a single rotation

$$\widetilde{C}(t) = U^\dagger \; C(\tau_0)^{-1/2} \; C(t) \; C(\tau_0)^{-1/2} \; U$$

- columns of U are eigenvectors of $C(\tau_0)^{-1/2}\, C(\tau_D)\, C(\tau_0)^{-1/2}$
- choose τ_0 and τ_D large enough so $\widetilde{C}(t)$ diagonal for $t > \tau_D$
- effective energies

$$\widetilde{m}_\alpha^{\text{eff}}(t) = \frac{1}{\Delta t} \ln\left(\frac{\widetilde{C}_{\alpha\alpha}(t)}{\widetilde{C}_{\alpha\alpha}(t+\Delta t)}\right)$$

  tend to N lowest-lying stationary state energies in a channel
- 2-exponential fits to $\widetilde{C}_{\alpha\alpha}(t)$ yield energies E_α and overlaps $Z_j^{(n)}$

Correlator matrix toy model

- **Theorem:** For every $t \geq 0$, let $\lambda_n(t)$ be the eigenvalues of an $N \times N$ Hermitian correlation matrix $C(t)$ ordered such that $\lambda_0 \geq \lambda_1 \geq \cdots \geq \lambda_{N-1}$, then

$$\lim_{t\to\infty} \lambda_n(t) = b_n e^{-E_n t}\left[1 + O(e^{-t\Delta_n})\right],$$
$$b_n > 0, \quad \Delta_n = \min_{m\neq n} |E_n - E_m|.$$

- Example: $N_e = 200$ eigenstates with energies

$$E_0 = 0.20, \qquad E_n = E_{n-1} + \frac{0.08}{\sqrt{n}}, \qquad n = 1, 2, \ldots, N_e - 1.$$

  for $N \times N$ correlator matrix, $N = 12$, overlaps

$$Z_j^{(n)} = \frac{(-1)^{j+n}}{1 + 0.05(j-n)^2}.$$

- toy model $N_e = 200$ with 12×12 correlator matrix $C(t)$

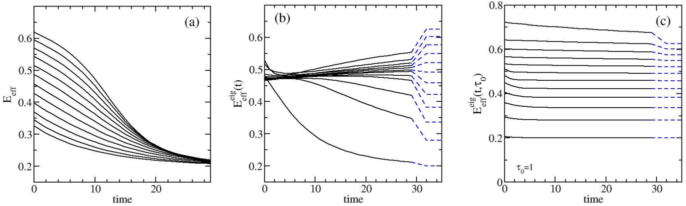

- left: effective energies of diagonal elements of correlator matrix
- middle: effective energies of eigenvalues of $C(t)$
- right: effective energies of eigenvalues of $C(\tau_0)^{-1/2}\ C(t)\ C(\tau_0)^{-1/2}$ for $\tau_0 = 1$

Building blocks for single-hadron operators

- building blocks: covariantly-displaced LapH-smeared quark fields
- stout links $\widetilde{U}_j(x)$
- Laplacian-Heaviside (LapH) smeared quark fields

$$\widetilde{\psi}_{a\alpha}(x) = \mathcal{S}_{ab}(x,y)\ \psi_{b\alpha}(y), \qquad \mathcal{S} = \Theta\left(\sigma_s^2 + \widetilde{\Delta}\right)$$

- 3d gauge-covariant Laplacian $\widetilde{\Delta}$ in terms of $\widetilde{U}$
- displaced quark fields:

$$q^A_{a\alpha j} = D^{(j)}\widetilde{\psi}^{(A)}_{a\alpha}, \qquad \overline{q}^A_{a\alpha j} = \widetilde{\overline{\psi}}^{(A)}_{a\alpha}\gamma_4\, D^{(j)\dagger}$$

- displacement $D^{(j)}$ is product of smeared links:

$$D^{(j)}(x,x') = \widetilde{U}_{j_1}(x)\ \widetilde{U}_{j_2}(x+d_2)\ \widetilde{U}_{j_3}(x+d_3)\dots\widetilde{U}_{j_p}(x+d_p)\delta_{x',\ x+d_{p+1}}$$

- to good approximation, LapH smearing operator is

$$\mathcal{S} = V_s V_s^\dagger$$

  - columns of matrix V_s are eigenvectors of $\widetilde{\Delta}$

Extended operators for single hadrons

- quark displacements build up orbital, radial structure

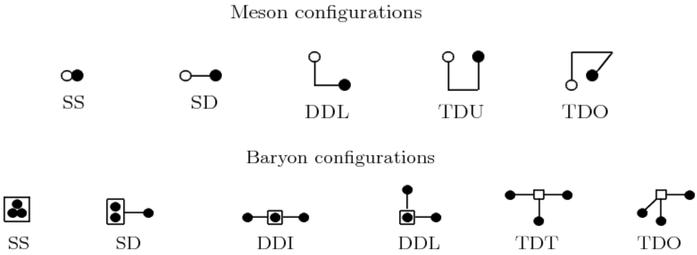

$$\overline{\Phi}^{AB}_{\alpha\beta}(\boldsymbol{p},t) = \sum_{\boldsymbol{x}} e^{i\boldsymbol{p}\cdot(\mathbf{x}+\frac{1}{2}(\boldsymbol{d}_\alpha+\boldsymbol{d}_\beta))}\delta_{ab}\ \overline{q}^{B}_{b\beta}(\boldsymbol{x},t)\ q^{A}_{a\alpha}(\boldsymbol{x},t)$$

$$\overline{\Phi}^{ABC}_{\alpha\beta\gamma}(\boldsymbol{p},t) = \sum_{\boldsymbol{x}} e^{i\boldsymbol{p}\cdot\mathbf{x}}\varepsilon_{abc}\ \overline{q}^{C}_{c\gamma}(\boldsymbol{x},t)\ \overline{q}^{B}_{b\beta}(\boldsymbol{x},t)\ \overline{q}^{A}_{a\alpha}(\boldsymbol{x},t)$$

- group-theory projections onto irreps of lattice symmetry group

$$\overline{M}_l(t) = c^{(l)*}_{\alpha\beta}\ \overline{\Phi}^{AB}_{\alpha\beta}(t) \qquad \overline{B}_l(t) = c^{(l)*}_{\alpha\beta\gamma}\ \overline{\Phi}^{ABC}_{\alpha\beta\gamma}(t)$$

- definite momentum $\boldsymbol{p}$, irreps of little group of $\boldsymbol{p}$

Importance of smeared fields

- effective masses of 3 selected nucleon operators shown
- noise reduction of displaced-operators from link smearing $n_\rho \rho = 2.5, n_\rho = 16$
- quark-field smearing $\sigma_s = 4.0, n_\sigma = 32$ reduces excited-state contamination

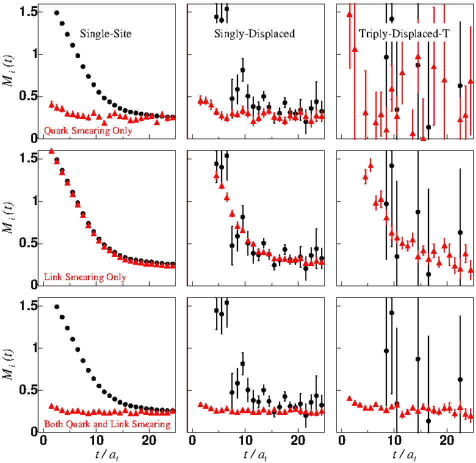

Two-hadron operators

- our approach: superposition of products of single-hadron operators of definite momenta

$$c^{I_{3a}I_{3b}}_{\boldsymbol{p}_a\lambda_a;\ \boldsymbol{p}_b\lambda_b}\ B^{I_aI_{3a}S_a}_{\boldsymbol{p}_a\Lambda_a\lambda_a i_a}\ B^{I_bI_{3b}S_b}_{\boldsymbol{p}_b\Lambda_b\lambda_b i_b}$$

- fixed total momentum $\boldsymbol{p} = \boldsymbol{p}_a + \boldsymbol{p}_b$, fixed $\Lambda_a, i_a, \Lambda_b, i_b$
- group-theory projections onto little group of $\boldsymbol{p}$ and isospin irreps
- crucial to know and fix all phases of single-hadron operators for all momenta
  - each class, choose reference direction $\boldsymbol{p}_{\rm ref}$
  - each $\boldsymbol{p}$, select one reference rotation $R^{\boldsymbol{p}}_{\rm ref}$ that transforms $\boldsymbol{p}_{\rm ref}$ into $\boldsymbol{p}$
- efficient creating large numbers of two-hadron operators
- generalizes to three, four, ... hadron operators

Quark line diagrams

- temporal correlations involving our two-hadron operators need
  - slice-to-slice quark lines (from all spatial sites on a time slice to all spatial sites on another time slice)
  - sink-to-sink quark lines

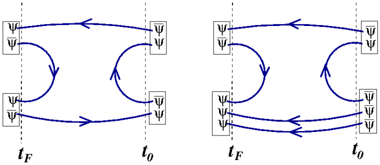

- isoscalar mesons also require sink-to-sink quark lines

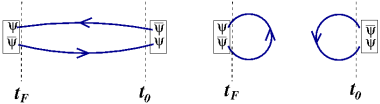

- solution: the stochastic LapH method!

Stochastic estimation of quark propagators

- do not need exact inverse of Dirac matrix $K[U]$
- introduce Z_4 noise vectors η in the LapH subspace

$$\eta_{\alpha k}(t), \qquad t = \text{time}, \ \alpha = \text{spin}, \ k = \text{eigenvector number}$$

- solve $K[U]X^{(r)} = \eta^{(r)}$ for each of N_R noise vectors $\eta^{(r)}$, then obtain a Monte Carlo estimate of all elements of K^{-1}

$$K_{ij}^{-1} \approx \frac{1}{N_R} \sum_{r=1}^{N_R} X_i^{(r)} \eta_j^{(r)*}$$

- variance reduction using noise dilution
- dilution introduces projectors $P^{(a)}$, then define

$$\eta^{[a]} = P^{(a)}\eta, \qquad X^{[a]} = K^{-1}\eta^{[a]}$$

to obtain Monte Carlo estimate with drastically reduced variance

$$K_{ij}^{-1} \approx \frac{1}{N_R} \sum_{r=1}^{N_R} \sum_a X_i^{(r)[a]} \eta_j^{(r)[a]*}$$

The effectiveness of stochastic LapH

- comparing use of lattice noise vs noise in LapH subspace
- N_D is number of solutions to $Kx = y$

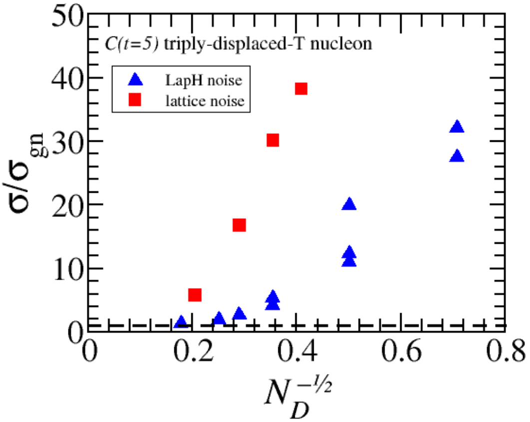

Correlators and quark line diagrams

- baryon correlator

$$C_{l\bar{l}} \approx \frac{1}{N_R} \sum_{r} \sum_{d_A d_B d_C} \mathcal{B}_l^{(r)[d_A d_B d_C]}(\varphi^A, \varphi^B, \varphi^C)\,\mathcal{B}_{\bar{l}}^{(r)[d_A d_B d_C]}(\varrho^A, \varrho^B, \varrho^C)^*$$

- express diagrammatically

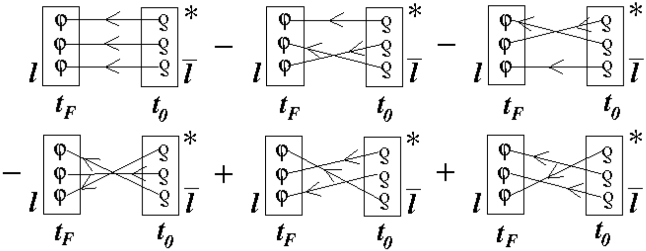

- meson correlator

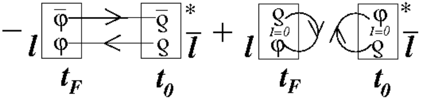

More complicated correlators

- two-meson to two-meson correlators (non isoscalar mesons)

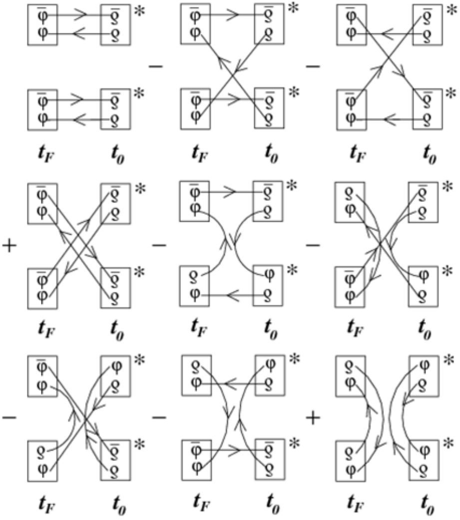

Quantum numbers in toroidal box

- periodic boundary conditions in cubic box
  - not all directions equivalent $\Rightarrow$ using J^{PC} is wrong!!

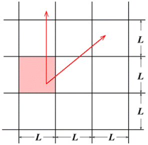

- label stationary states of QCD in a periodic box using irreps of cubic space group even in continuum limit
  - zero momentum states: little group O_h

$$A_{1a}, A_{2ga}, E_a, T_{1a}, T_{2a}, \quad G_{1a}, G_{2a}, H_a, \qquad a = g, u$$

  - on-axis momenta: little group C_{4v}

$$A_1, A_2, B_1, B_2, E, \quad G_1, G_2$$

  - planar-diagonal momenta: little group C_{2v}

$$A_1, A_2, B_1, B_2, \quad G_1, G_2$$

  - cubic-diagonal momenta: little group C_{3v}

$$A_1, A_2, E, \quad F_1, F_2, G$$

- include G parity in some meson sectors (superscript $+$ or $-$)

Spin content of cubic box irreps

- numbers of occurrences of Λ irreps in J subduced

J	A_1	A_2	E	T_1	T_2
0	1	0	0	0	0
1	0	0	0	1	0
2	0	0	1	0	1
3	0	1	0	1	1
4	1	0	1	1	1
5	0	0	1	2	1
6	1	1	1	1	2
7	0	1	1	2	2

J	G_1	G_2	H	J	G_1	G_2	H
$\frac{1}{2}$	1	0	0	$\frac{9}{2}$	1	0	2
$\frac{3}{2}$	0	0	1	$\frac{11}{2}$	1	1	2
$\frac{5}{2}$	0	1	1	$\frac{13}{2}$	1	2	2
$\frac{7}{2}$	1	1	1	$\frac{15}{2}$	1	1	3

Ensembles and run parameters

- focusing on two Monte Carlo ensembles
  - $(32^3|240)$: 412 configs $32^3 \times 256$, $m_\pi \approx 240$ MeV, $m_\pi L \sim 4.4$
  - $(24^3|390)$: 551 configs $24^3 \times 128$, $m_\pi \approx 390$ MeV, $m_\pi L \sim 5.7$
- anisotropic improved gluon action, clover quarks (stout links)
- QCD coupling $\beta = 1.5$ such that $a_s \sim 0.12$ fm, $a_t \sim 0.035$ fm
- strange quark mass $m_s = -0.0743$ nearly physical (using kaon)
- work in $m_u = m_d$ limit so $SU(2)$ isospin exact
- generated using RHMC, configs separated by 20 trajectories

- stout-link smearing in operators $\xi = 0.10$ and $n_\xi = 10$
- LapH smearing cutoff $\sigma_s^2 = 0.33$ such that
  - $N_v = 112$ for 24^3 lattices
  - $N_v = 264$ for 32^3 lattices
- source times:
  - 4 widely-separated t_0 values on 24^3
  - 8 t_0 values used on 32^3 lattice

$I = 1,\ S = 0,\ T_{1u}^{+}$ channel

- effective energies $\widetilde{m}^{\rm eff}(t)$ for levels 0 to 24 $(32^3|240)$
- energies obtained from two-exponential fits (B. Fahy, PhD thesis)

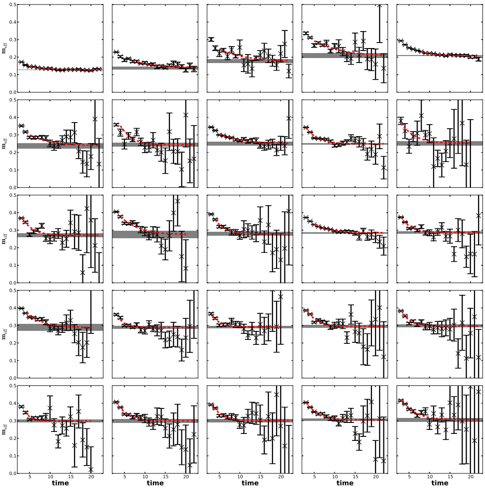

$I = 1,\ S = 0,\ T_{1u}^{+}$ energy extraction, continued

- effective energies $\widetilde{m}^{\rm eff}(t)$ for levels 25 to 49
- energies obtained from two-exponential fits

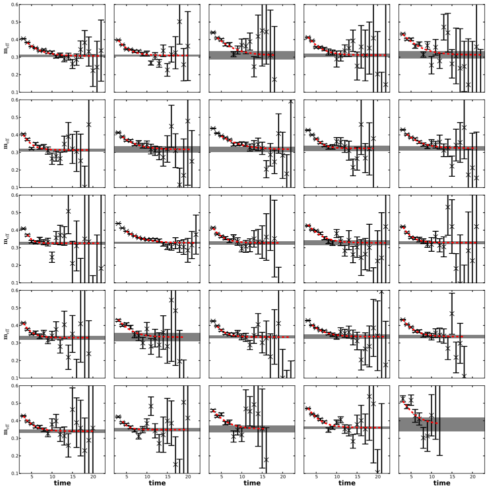

Level identification

- overlaps for various operators

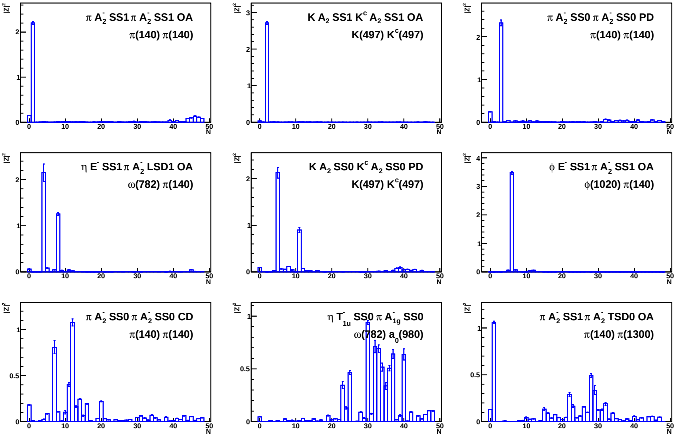

Staircase of energy levels

- stationary state energies $I = 1,\ S = 0,\ T_{1u}^{+}$ channel on $(32^3 \times 256)$ anisotropic lattice

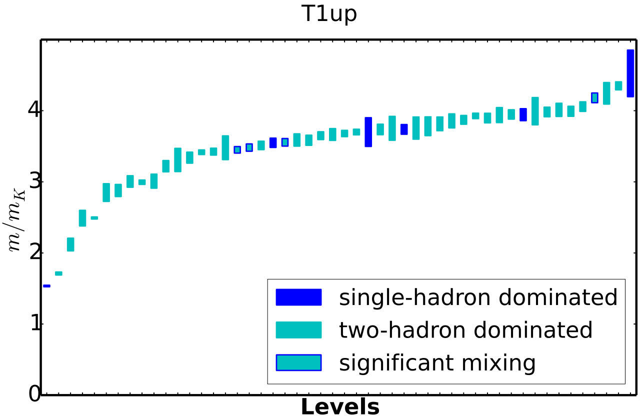

Summary and comparison with experiment

- right: energies of $\overline{q}q$-dominant states as ratios over m_K for $(32^3|240)$ ensemble
- left: experiment (masses and widths)

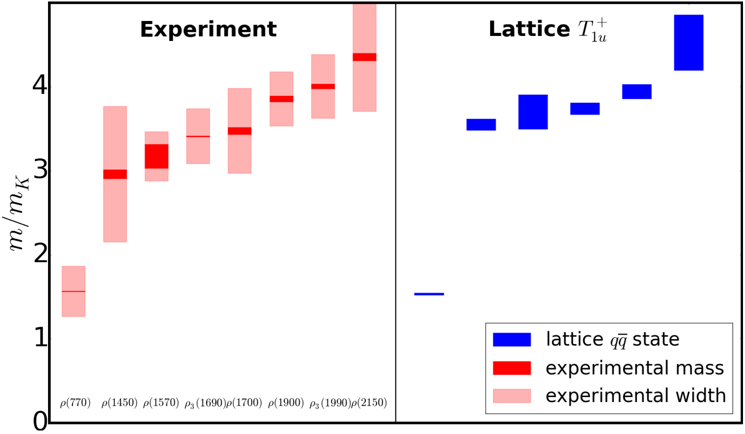

Issues

- infinite-volume resonance parameters from finite-volume energies
  - Luscher method too cumbersome, restrictive in applicability
  - use of hadron effective Hamiltonian techniques
- address presence of 3 and 4 meson states
- in other channels, address scalar particles in spectrum
  - scalar probe states need vacuum subtractions
  - hopefully can neglect due to OZI suppression

Bosonic $I = 1,\ S = 0,\ A_{1u}^{-}$ channel

- finite-volume stationary-state energies: “staircase” plot
- $32^3 \times 256$ lattice for $m_\pi \sim 240$ MeV
- use of single- and two-meson operators only
- blue: levels of max ovelaps with SH optimized operators

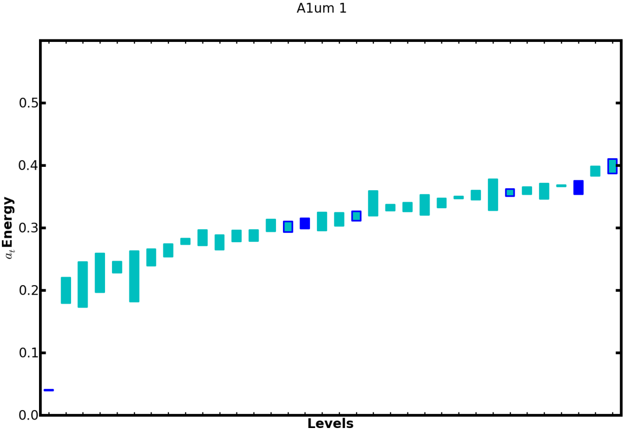

Bosonic $I = 1,\ S = 0,\ E_u^+$ channel

- finite-volume stationary-state energies: "staircase" plot
- $32^3 \times 256$ lattice for $m_\pi \sim 240$ MeV
- use of single- and two-meson operators only
- blue: levels of max ovelaps with SH optimized operators

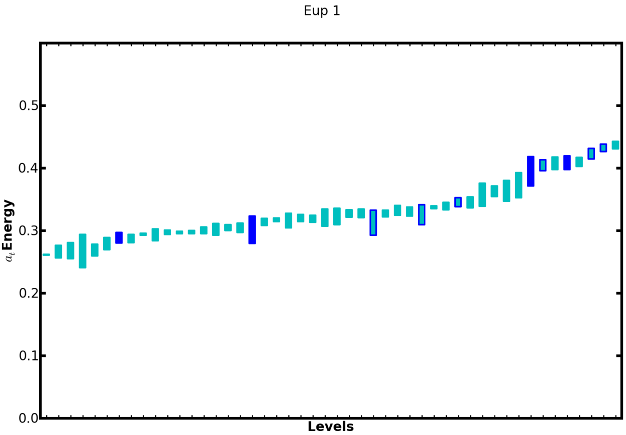

Bosonic $I = 1,\ S = 0,\ T_{1g}^-$ channel

- finite-volume stationary-state energies: “staircase” plot
- $32^3 \times 256$ lattice for $m_\pi \sim 240$ MeV
- use of single- and two-meson operators only
- blue: levels of max ovelaps with SH optimized operators

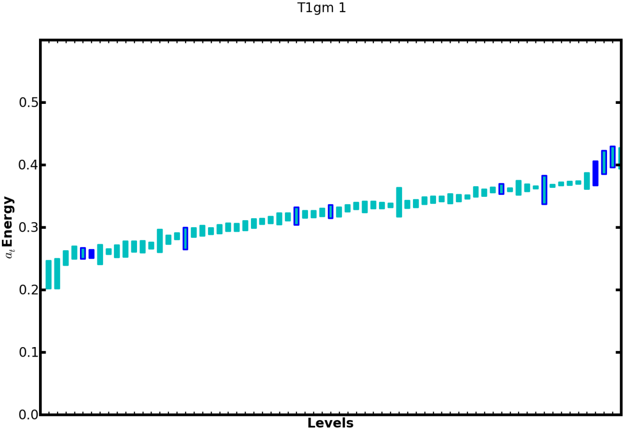

Bosonic $I = 1,\ S = 0,\ T_{1u}^{-}$ channel

- finite-volume stationary-state energies: “staircase” plot
- $32^3 \times 256$ lattice for $m_\pi \sim 240$ MeV
- use of single- and two-meson operators only
- blue: levels of max ovelaps with SH optimized operators

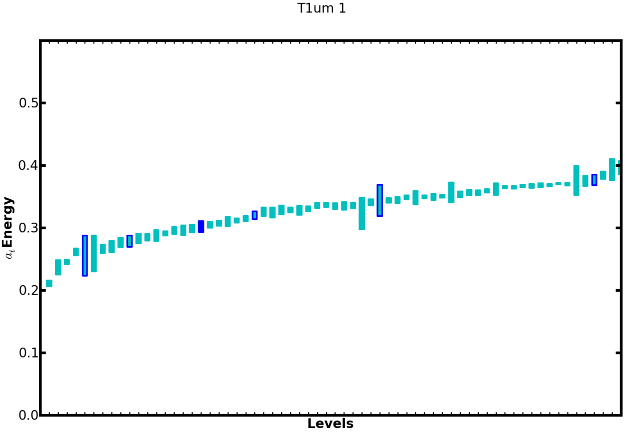

Bosonic $I = \frac{1}{2},\ S = 1,\ T_{1u}$ channel

- kaon channel: effective energies $\widetilde{m}^{\text{eff}}(t)$ for levels 0 to 8
- results for $32^3 \times 256$ lattice for $m_\pi \sim 240$ MeV
- two-exponential fits (Y.C. Jhang, PhD thesis)

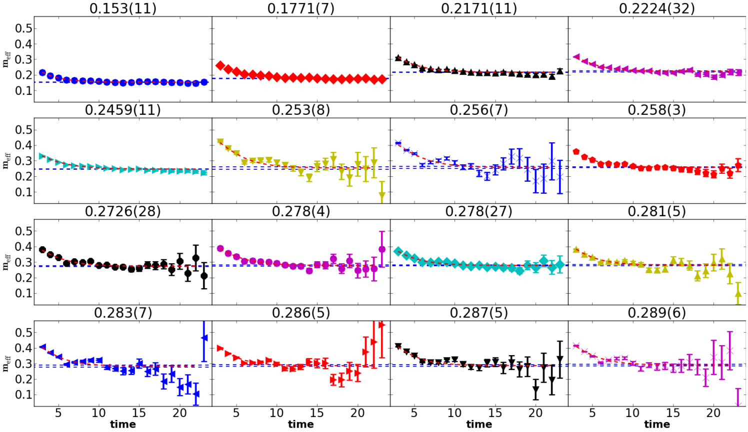

Bosonic $I = \frac{1}{2},\ S = 1,\ T_{1u}$ channel

- effective energies $\widetilde{m}^{\text{eff}}(t)$ for levels 9 to 17
- results for $32^3 \times 256$ lattice for $m_\pi \sim 240$ MeV
- two-exponential fits

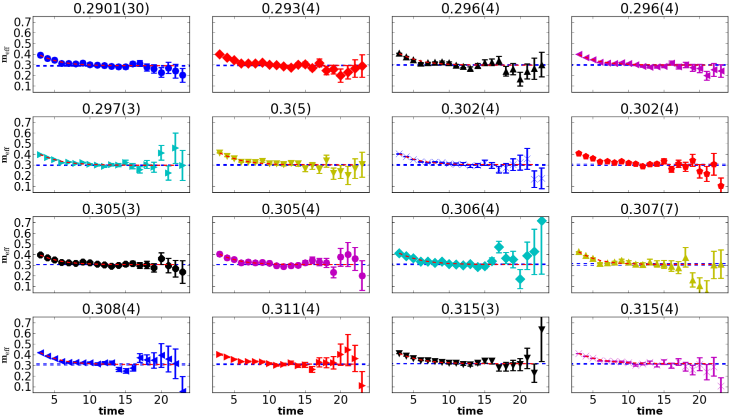

Bosonic $I = \frac{1}{2},\ S = 1,\ T_{1u}$ channel

- effective energies $\widetilde{m}^{\rm eff}(t)$ for levels 18 to 23
- dashed lines show energies from single exponential fits

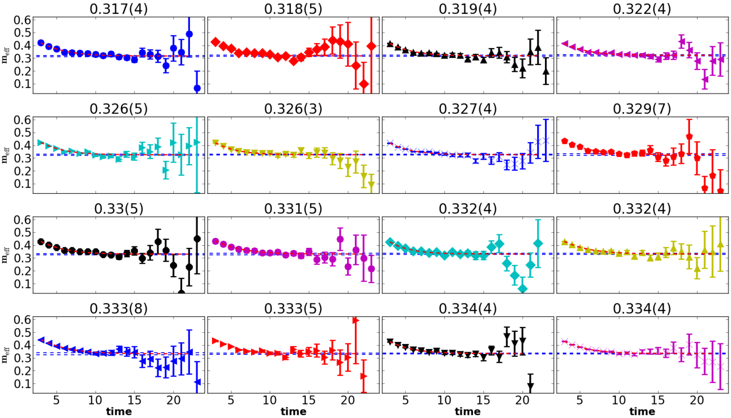

Bosonic $I = \frac{1}{2},\ S = 1,\ T_{1u}$ channel

- finite-volume stationary-state energies: "staircase" plot
- $32^3 \times 256$ lattice for $m_\pi \sim 240$ MeV
- use of single- and two-meson operators only
- blue: levels of max ovelaps with SH optimized operators

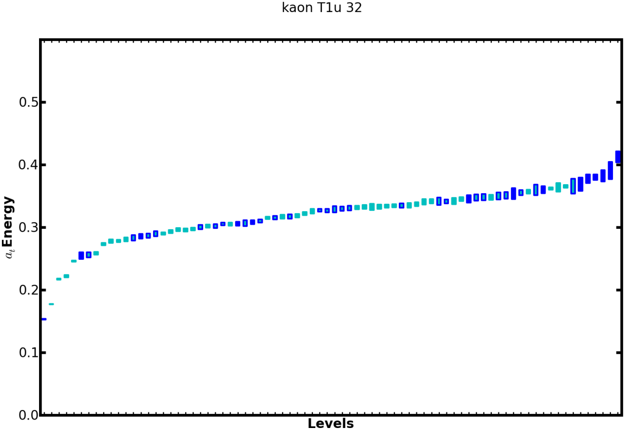

Scattering phase shifts in lattice QCD timeline

- DeWitt 1956: finite-volume energies related to scattering phase shifts
- Lüscher 1984: quantum mechanics in a box
- Rummukainen and Gottlieb 1995: nonzero total momenta
- Kim, Sachrajda, and Sharpe 2005: field theoretic derivation
- explosion of papers since then
- generalized to arbitrary spin, multiple channels

Scattering phase shifts from finite-volume energies

- correlator of two-particle operator σ in finite volume

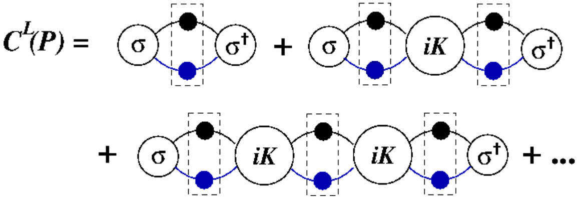

- Bethe-Salpeter kernel

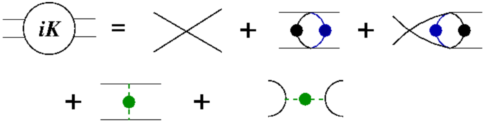

- $C^{\infty}(P)$ has branch cuts where two-particle thresholds begin
- momentum quantization in finite volume: cuts $\rightarrow$ series of poles
- C^{L} poles: two-particle energy spectrum of finite volume theory

- finite-volume momentum sum is infinite-volume integral plus correction $\mathcal{F}$

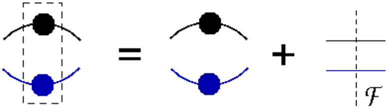

- define the following quantities: A, A', invariant scattering amplitude $i\mathcal{M}$

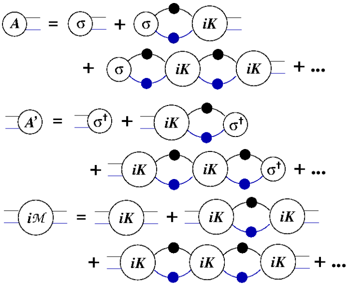

Phase shifts from finite-volume energies (con't)

- subtracted correlator $C_{\text{sub}}(P) = C^L(P) - C^\infty(P)$ given by

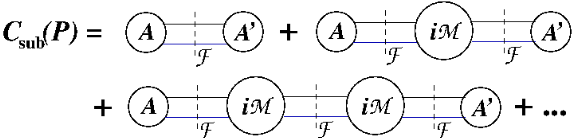

- sum geometric series

$$C_{\text{sub}}(P) = A\,\mathcal{F}(1 - i\mathcal{M}\mathcal{F})^{-1}\,A'.$$

- poles of $C_{\text{sub}}(P)$ are poles of $C^L(P)$ from $\det(1 - i\mathcal{M}\mathcal{F}) = 0$
- key tool: for $g_c(\boldsymbol{p})$ spatially contained and regular

$$\frac{1}{L^3}\sum_{\boldsymbol{p}} g_c(\boldsymbol{p}) = \int \frac{d^3k}{(2\pi)^3}\, g_c(\mathbf{k}) + O(e^{-mL})$$

$$\frac{1}{L^3}\sum_{\boldsymbol{p}} \frac{g_c(\boldsymbol{p}^2)}{(\boldsymbol{p}^2 - a^2)} = \frac{1}{L^3}\sum_{\boldsymbol{p}} \frac{g_c(a^2)}{(\boldsymbol{p}^2 - a^2)} + \int \frac{d^3k}{(2\pi)^3} \frac{g_c(\boldsymbol{p}^2) - g(a^2)}{(\boldsymbol{p}^2 - a^2)} + O(e^{-mL})$$

Phase shifts from finite-volume energies (con't)

- work in spatial L^3 volume with periodic b.c.
- total momentum $\boldsymbol{P} = (2\pi/L)\boldsymbol{d}$, where $\boldsymbol{d}$ vector of integers
- masses m_1 and m_2 of particle 1 and 2
- calculate lab-frame energy E of two-particle interacting state in lattice QCD
- boost to center-of-mass frame by defining:

$$\begin{aligned}
E_{\rm cm} &= \sqrt{E^2 - \boldsymbol{P}^2}, \qquad \gamma = \frac{E}{E_{\rm cm}}, \\
\boldsymbol{q}^2_{\rm cm} &= \frac{1}{4}E^2_{\rm cm} - \frac{1}{2}(m_1^2 + m_2^2) + \frac{(m_1^2 - m_2^2)^2}{4E^2_{\rm cm}}, \\
u^2 &= \frac{L^2 \boldsymbol{q}^2_{\rm cm}}{(2\pi)^2}, \qquad \boldsymbol{s} = \left(1 + \frac{(m_1^2 - m_2^2)}{E^2_{\rm cm}}\right)\boldsymbol{d}
\end{aligned}$$

- E related to S matrix (and phase shifts) by

$$\det[1 + F^{(\boldsymbol{s},\gamma,u)}(S - 1)] = 0,$$

  where F matrix defined next slide

Phase shifts from finite-volume energies (con't)

- F matrix in JLS basis states given by

$$F^{(\boldsymbol{s},\gamma,u)}_{J'm_{J'}L'S'a';\; Jm_JLSa} = \frac{\rho_a}{2}\delta_{a'a}\delta_{S'S}\Big\{\delta_{J'J}\delta_{m_{J'}m_J}\delta_{L'L}$$

$$+W^{(\boldsymbol{s},\gamma,u)}_{L'm_{L'};\; Lm_L}\langle J'm_{J'}|L'm_{L'},Sm_S\rangle\langle Lm_L,Sm_S|Jm_J\rangle\Big\},$$

- total angular mom J, J', orbital mom L, L', intrinsic spin S, S'
- a, a' channel labels
- $\rho_a = 1$ distinguishable particles, $\rho_a = \frac{1}{2}$ identical

$$W^{(\boldsymbol{s},\gamma,u)}_{L'm_{L'};\; Lm_L} = \frac{2i}{\pi\gamma u^{l+1}}\mathcal{Z}_{lm}(\boldsymbol{s},\gamma,u^2)\int d^2\Omega\; Y^*_{L'm_{L'}}(\Omega)Y^*_{lm}(\Omega)Y_{Lm_L}(\Omega)$$

- Rummukainen-Gottlieb-Lüscher (RGL) shifted zeta functions $\mathcal{Z}_{lm}$ defined next slide
- $F^{(\boldsymbol{s},\gamma,u)}$ diagonal in channel space, mixes different J, J'
- recall S diagonal in angular momentum, but off-diagonal in channel space

RGL shifted zeta functions

- compute $\mathcal{Z}_{lm}$ using

$$\mathcal{Z}_{lm}(\boldsymbol{s},\gamma,u^2) = \sum_{\boldsymbol{n}\in\mathbb{Z}^3} \frac{\mathcal{Y}_{lm}(\boldsymbol{z})}{(\boldsymbol{z}^2-u^2)} e^{-\Lambda(\boldsymbol{z}^2-u^2)} + \delta_{l0}\frac{\gamma\pi}{\sqrt{\Lambda}} F_0(\Lambda u^2)$$

$$+\frac{i^l\gamma}{\Lambda^{l+1/2}} \int_0^1 dt \left(\frac{\pi}{t}\right)^{l+3/2} e^{\Lambda t u^2} \sum_{\substack{\boldsymbol{n}\in\mathbb{Z}^3\\ \boldsymbol{n}\neq 0}} e^{\pi i \boldsymbol{n}\cdot\boldsymbol{s}} \mathcal{Y}_{lm}(\mathbf{w})\ e^{-\pi^2\mathbf{w}^2/(t\Lambda)}$$

- where

$$\boldsymbol{z} = \boldsymbol{n} - \gamma^{-1}\left[\tfrac{1}{2} + (\gamma-1)s^{-2}\boldsymbol{n}\cdot\boldsymbol{s}\right]\boldsymbol{s},$$

$$\mathbf{w} = \boldsymbol{n} - (1-\gamma)s^{-2}\boldsymbol{s}\cdot\boldsymbol{n}\boldsymbol{s}, \qquad \mathcal{Y}_{lm}(\mathbf{x}) = |\mathbf{x}|^l\ Y_{lm}(\widehat{\mathbf{x}})$$

$$F_0(x) = -1 + \frac{1}{2}\int_0^1 dt\ \frac{e^{tx}-1}{t^{3/2}}$$

- choose $\Lambda \approx 1$ for convergence of the summation
- integral done Gauss-Legendre quadrature
- $F_0(x)$ given in terms of Dawson or erf function

Block diagonalization of F matrix

- quantization condition is large determinant relation:

$$\det[1 + F^{(\boldsymbol{s},\gamma,u)}(S-1)] = 0$$

- define the matrix

$$B^{(R)}_{J'm_{J'}L'S'a';\; Jm_JLSa} = \delta_{J'J}\delta_{L'L}\delta_{S'S}\delta_{a'a}D^{(J)*}_{m_{J'}m_J}(R)$$

- can show that under lattice symmetry operator R,

$$F^{(R\boldsymbol{s},\gamma,u)} = B^{(R)}\; F^{(\boldsymbol{s},\gamma,u)}\; B^{(R)\dagger}$$

- can block diagonalize F by diagonalizing $D^{(J)}_{m'm}(R)$ for each J
- change of basis: little group irrep Λ, row λ, n occurrence of Λ in $D^{(J)}_{m'm}(R)$

$$|\Lambda\lambda nJLSa\rangle = \sum_{m_J} c^{\Lambda\lambda n}_{Jm_J}|Jm_JLSa\rangle$$

- F diagonal in Λ, λ, but not in n_Λ
- can now focus on the matrix elements:

$$F^{(\boldsymbol{s},\gamma,u)(\Lambda,\lambda)}_{J'n'L'S'a';\; JnLSa}$$

P-wave $I = 1$ $\pi\pi$ scattering

- for P-wave phase shift $\delta_1(E_{\rm cm})$ for $\pi\pi$ $I = 1$ scattering
- define

$$w_{lm} = \frac{\mathcal{Z}_{lm}(\boldsymbol{s}, \gamma, u^2)}{\gamma \pi^{3/2} u^{l+1}}$$

$\boldsymbol{d}$	Λ	$\cot \delta_1$
(0,0,0)	T_{1u}^+	$\mathrm{Re}\ w_{0,0}$
(0,0,1)	A_1^+	$\mathrm{Re}\ w_{0,0} + \frac{2}{\sqrt{5}} \mathrm{Re}\ w_{2,0}$
	E^+	$\mathrm{Re}\ w_{0,0} - \frac{1}{\sqrt{5}} \mathrm{Re}\ w_{2,0}$
(0,1,1)	A_1^+	$\mathrm{Re}\ w_{0,0} + \frac{1}{2\sqrt{5}} \mathrm{Re}\ w_{2,0} - \sqrt{\frac{6}{5}} \mathrm{Im}\ w_{2,1} - \sqrt{\frac{3}{10}} \mathrm{Re}\ w_{2,2},$
	B_1^+	$\mathrm{Re}\ w_{0,0} - \frac{1}{\sqrt{5}} \mathrm{Re}\ w_{2,0} + \sqrt{\frac{6}{5}} \mathrm{Re}\ w_{2,2},$
	B_2^+	$\mathrm{Re}\ w_{0,0} + \frac{1}{2\sqrt{5}} \mathrm{Re}\ w_{2,0} + \sqrt{\frac{6}{5}} \mathrm{Im} w_{2,1} - \sqrt{\frac{3}{10}} \mathrm{Re}\ w_{2,2}$
(1,1,1)	A_1^+	$\mathrm{Re}\ w_{0,0} + 2\sqrt{\frac{6}{5}} \mathrm{Im}\ w_{2,2}$
	E^+	$\mathrm{Re}\ w_{0,0} - \sqrt{\frac{6}{5}} \mathrm{Im}\ w_{2,2}$

Finite-volume $\pi\pi$ $I = 1$ energies

- $\pi\pi$-state energies for various $\boldsymbol{d}^2$

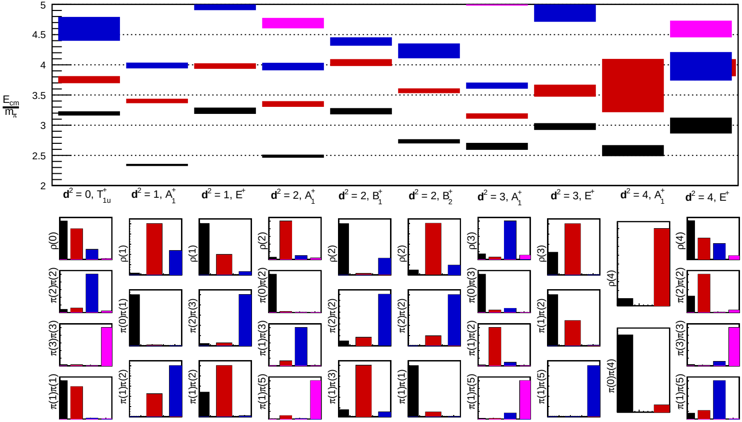

$I = 1$ $\pi\pi$ scattering phase shift and width of the ρ

- results $32^3 \times 256$, $m_\pi \approx 240$ MeV:

$$g_{\rho\pi\pi} = 5.99(26), \; m_\rho/m_\pi = 3.350(24), \; \chi^2/\mathrm{dof} = 1.04$$

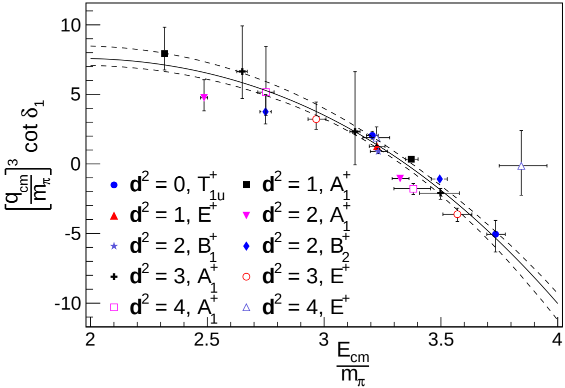

- fit $\quad g_{\rho\pi\pi}^2 q_{\mathrm{cm}}^3 \cot(\delta_1) = 6\pi E_{\mathrm{cm}}(m_\rho^2 - E_{\mathrm{cm}}^2)$

$I = 1$ $\pi\pi$ scattering phase shift and width of the ρ

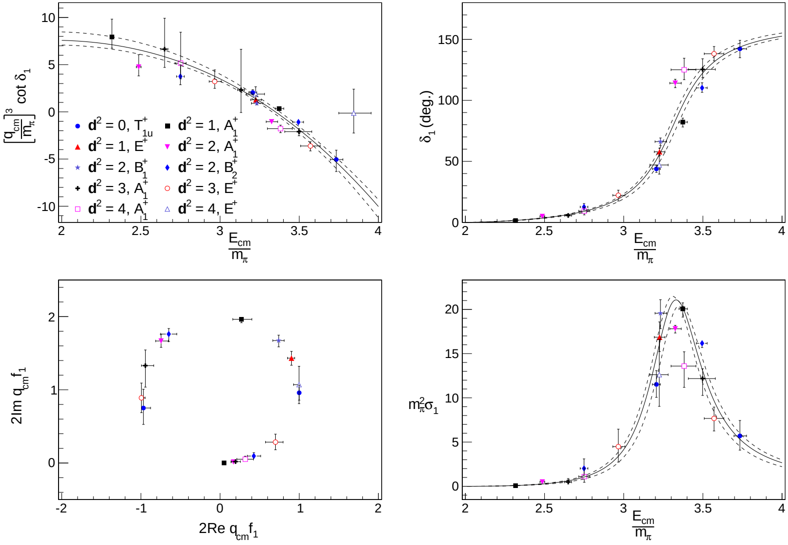

$I = 1$ $\pi\pi$ scattering phase shift and width of the ρ

- compendium of results for $g_{\rho\pi\pi}$

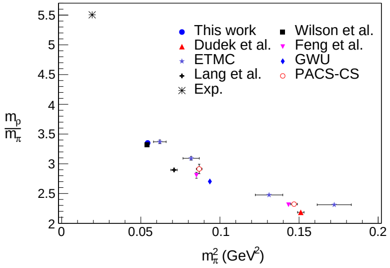

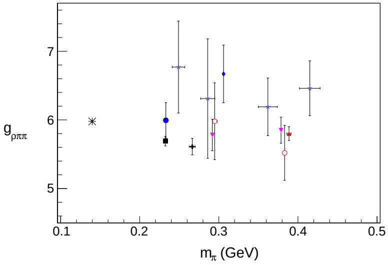

Effective Hamiltonian method

- relating finite-volume energies to resonance parameters via "Lüscher method" very complicated
- alternative: use an effective hadron Hamiltonian matrix
  - Wu et al, PRC **90**, 055206 (2014)
- use single and two-particle states as basis states
- interaction terms from symmetry + assumed form wrt momenta
- parameters of Hamiltonian determined from fits to finite-volume spectra
- Lippmann-Schwinger (or other methods) to extract infinite-volume resonances

Tetraquark operators

- determine impact on spectrum when tetraquark operators included
- single-site and displaced quarks

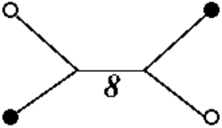

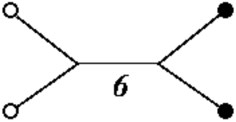

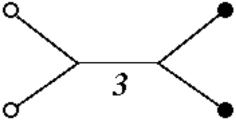

References

- S. Basak et al., *Group-theoretical construction of extended baryon operators in lattice QCD*, Phys. Rev. D **72**, 094506 (2005).
- S. Basak et al., *Lattice QCD determination of patterns of excited baryon states*, Phys. Rev. D **76**, 074504 (2007).
- C. Morningstar et al., *Improved stochastic estimation of quark propagation with Laplacian Heaviside smearing in lattice QCD*, Phys. Rev. D **83**, 114505 (2011).
- C. Morningstar et al., *Extended hadron and two-hadron operators of definite momentum for spectrum calculations in lattice QCD*, Phys. Rev. D **88**, 014511 (2013).
- J. Bulava et al., *$I = 1$ and $I = 2$ $\pi\pi$ scattering phase shifts from $N_f = 2 + 1$ lattice QCD*, submitted to Nucl. Phys. B. (2016).

Conclusion

- excited states are difficult!
- crucial role of interpolating operators for excited-state studies in lattice QCD
- large number of finite-volume energies in large number of channels now possible
- stochastic LapH method works very well
  - allows evaluation of all needed quark-line diagrams
- scattering phase shifts can be computed
- infinite-volume resonance parameters from finite-volume energies $\longrightarrow$ need for simpler effective Hamiltonian/field theory techniques
- role of tetraquark operators to be studied